Polymer Chemistry

ROYAL SOCIETY OF CHEMISTRY

PAPER

View Article Online
View Journal | View Issue

Cite this: *Polym. Chem.*, 2020, **11**, 3066

Synthesis of conjugated polymers *via* cyclopentannulation reaction: promising materials for iodine adsorption†

Noorullah Baig,[a,b] Suchetha Shetty,[a,b] Saleh Al-Mousawi[c] and Bassam Alameddine *[a,b]

Received 21st February 2020,
Accepted 3rd April 2020

DOI: 10.1039/d0py00286k

rsc.li/polymers

A new class of conjugated polymers is prepared by means of a versatile palladium-catalyzed cyclopentannulation reaction using a series of specially designed diethynyl aryl synthons with the commercially available 9,10-dibromoanthracene **DBA** monomer. The target polymers, **CPP1–3**, display high solubility and excellent chemical stability, which allow their structural and photophysical characterization by various instrumental analysis techniques such as gel permeation chromatography (GPC), and ^{1}H- and ^{13}C-nuclear magnetic resonance (NMR), Fourier transform infrared (FTIR), UV-vis absorption, and emission spectroscopy. GPC chromatograms of **CPP1–3** display a high relative weight-average (M_w) molecular weight in the range of 15.8 to 34.3 kDa with a polydispersity index ($Đ$ = M_w/M_n) of ~2.5. Investigation of the iodine adsorption properties of **CPP1–3** reveals their high uptake, namely ~200 wt% for **CPP2**, whose sorption property was sustained even after its reuse several times.

Introduction

The design of new conjugated polymers has become one of the chief topics of interest for scientific endeavors because of the importance of this latter class of materials in diverse applications, namely, light-emitting diodes (LEDs),[1–3] organic solar cells,[4–7] field-effect transistors (FETs),[8–16] sensors,[17] optical switches,[18–22] batteries,[23] and thermoelectrics.[24] In addition to the hitherto mentioned applications, conjugated microporous polymers (CMP) have become exceptionally eminent due to many reasons, notably their extended π-conjugation skeleton, high stability, synthesis versatility, large surface area, and excellent gas sorption properties.[25]

The total world energy demand is increasing rapidly as a result of the rise in global population and economic growth. It is estimated that the energy consumption will reach 778 Etta Joule by 2035.[26] In the meantime, the quest for a sustainable, efficient, low-emission energy source continues to be a global interdisciplinary research challenge.[27] Wind power and solar energy are often considered potential alternatives for our current fossil-fuel based energy economy, but their sporadic nature of energy production leads to reliability concerns.[28] Nuclear energy is considered to be a possible option for continuous energy production.[29] Nevertheless, the successful mass production of power from nuclear fission is accompanied by the emission of several radioactive gases, such as, $^{14}CO_2$, ^{85}Kr, ^{3}H, ^{123}I, ^{125}I, and $^{127–140}$I.[30] In addition to the hitherto mentioned radioactive iodine, hydrogen iodide (HI) and alkyl halides are also considered hazardous due to their large heat release, involvement in metabolic processes, and long half-lives (*e.g.*, $t_{1/2}$ = 15.7 × 10^6 years for ^{129}I).[31,32] Consequently, in view of its threat to human health and for being a mutation source of plants and animals, there is a need for effective and longer-lasting solutions to capture and store the radioactive iodine species.[33–35] Amongst the most efficient and cost-effective adsorption technologies, porous adsorbents, such as organic cages, silica gel, zeolites, activated carbon, and metal organic frameworks, have been tested for iodine capture.[36–40]

Various conjugated polymers have been reported with structures ranging from linear,[14,41] hypercrosslinked,[42] organic frameworks,[25,43] to polycyclic aromatic hydrocarbons.[44–48] Nevertheless, the rigidity and stiffness of these polymers make them poorly soluble, which can be circumvented by the introduction of aliphatic side chains in order to improve their solubility in common organic solvents. However, the insertion of long peripheral chains hampers microporosity since these latter block the intrinsic pores.[49] An alternative strategy to improve the solubility of conjugated polymers would be the

[a]*Department of Mathematics and Natural Sciences, Gulf University for Science and Technology (GUST), Kuwait. E-mail: alameddine.b@gust.edu.kw*
[b]*Functional Materials Group – CAMB, GUST, Kuwait*
[c]*Department of Chemistry, University of Kuwait, Kuwait*
†Electronic supplementary information (ESI) available. See DOI: 10.1039/d0py00286k

insertion of spiro-centers that result in the formation of contorted structures, which prevents any aggregation caused by π–π stacking.[50–52] Herein we describe the synthesis of three conjugated organic polymers **CPP1–3** from 9,10-dibromoanthracene **DBA** with various contorted aryl dialkyne comonomers **3a–c** *via* a versatile palladium-catalyzed cyclopentannulation reaction.[53,54] It is worth mentioning that the target polymers were obtained in excellent yields and were found to be highly soluble in common organic solvents. Hence, **CPP1–3** were characterized by GPC, NMR, FTIR, UV-vis absorption and emission spectroscopy. In addition, the target polymers were investigated for iodine uptake applications.

Experimental

Materials

All the reactions were carried out under an inert atmosphere using dry argon. All chemical reagents were used without further purification as purchased from Aldrich, Merck, and HiMedia unless otherwise specified. The triptycene nonaflate **2c** was synthesized following the literature.[55] The solvents, namely, hexane, DCM, THF, benzene, toluene, diisopropylamine, DMSO, and acetone, were dried and deoxygenated by bubbling with argon gas for 30 minutes. Thin-layer chromatography (TLC) was performed on aluminum sheets coated with silica gel 60 F254 and revealed using a UV lamp.

Instruments

NMR (^{1}H: 600 MHz, ^{13}C: 150 MHz) spectra were recorded on a Bruker BioSpin GmbH 600 MHz spectrometer using CD_2Cl_2/$CDCl_3$ as a solvent with the chemical shifts (δ) given in ppm and referred to tetramethylsilane (TMS). Electron impact high-resolution mass spectra (EI-HRMS) were recorded on a Themo Fisher DFS analyzer with a standard PFK (perfluorokerosene) as lock mass. The analysed data were converted to accurate mass employing X-Calibur accurate mass calculation software. UV-Vis spectra were recorded on a Shimadzu UV1800 spectrophotometer. Photoluminescence (PL) spectra were recorded on an Agilent G9800 Cary Eclipse Fluorescence spectrophotometer. An Agilent Gel Permeation Chromatography (GPC/SEC) system equipped with two columns (PL mixed-C) and calibrated against twelve monodisperse polystyrene (PS) standards, using THF as the eluent at a flow rate of 1.0 mL min^{-1}, was employed to determine the relative weight-average (M_w), number-average (M_n) molecular weights, and polydispersity index ($Đ = M_w/M_n$) of all the reported polymers. FT-IR spectra were recorded on an FT/IR-6300 type A instrument using a KBr matrix.

Synthesis

Synthesis of 3a (procedure A). A Schlenk tube was charged under argon with 1-(*tert*-butyl)-4-ethynylbenzene **1a** (0.25 mL, 1.4 mmol, 4.7 eq.), 2,7-dibromo-9,9-dimethyl-9*H*-fluorene **2a** (105 mg, 0.3 mmol, 1 eq.), $Pd_2(dba)_3$ (1.6 mg, 1.8 μmol, 6 mol%), PPh_3 (1 mg, 3.6 μmol), and CuI (1 mg, 6.0μ mol) in 2 mL of degassed diisopropylamine (iPr_2NH) and the solution was refluxed for 2 days. The resulting solid was filtered and washed exhaustively with petroleum ether yielding a pale pink solid (140 mg, 93%). ^{1}H NMR (600 MHz, CD_2Cl_2, ppm): δ 7.76 (d, 2H, J = 7.8 Hz, ArH), 7.66 (s, 2H, ArH), 7.56 (dd, 2H, J = 7.8, 6.6 Hz, ArH) 7.52 (m, 4H, J = 3.6 Hz, ArH) 7.45 (m, 4H, ArH), 1.55 (s, 6H, –CH_3),1.37 (s, 18H, –CH_3). ^{13}C NMR (150 MHz, CD_2Cl_2, ppm): δ 154.66, 152.35, 139.20, 131.80, 131.30, 126.50, 126.09, 122.94, 120.84, 90.44, 89.98, 47.47, 35.29, 31.50, 27.32. EI-HRMS: m/z calculated for $M^{\bullet+}$ $C_{39}H_{38}$ 506.2974 found 506.2975.

Synthesis of 3b. 3b was prepared following procedure A with 1-(*tert*-butyl)-4-ethynylbenzene **1a** (0.25 mL, 1.4 mmol, 4.7 eq.), 2,7-dibromo-9,9′-spirobifluorene **2b** (140 mg, 0.3 mmol, 1 eq.), $Pd_2(dba)_3$ (1.5 mg, 1.8 μmol, 6 mol%), PPh_3 (1 mg, 3.6 μmol), and CuI (1 mg, 6.0 μmol) in 2 mL of degassed diisopropylamine (iPr_2NH). Pale yellow solid (282 mg, 100%). ^{1}H NMR (600 MHz, CD_2Cl_2, ppm): δ 7.95 (d, 2H, J = 7.8 Hz, ArH), 7.90 (d, 2H, J = 7.8 Hz, ArH), 7.60 (dd, 2H, J = 7.8, 6.6 Hz, ArH) 7.46 (t, 2H, J = 7.8 Hz, ArH), 7.36 (bs, 8H, ArH), 7.20 (t, 2H, J = 7.8 Hz, ArH), 6.92 (s, 2H, ArH), 6.80 (d, 2H, J = 7.8 Hz, ArH), 1.32 (s, 18H, –CH_3). ^{13}C NMR (150 MHz, CD_2Cl_2, ppm): δ 151.74, 149.26, 147.77, 141.85, 141.10, 131.36, 131.08, 128.10, 127.99, 126.93, 125.39, 123.89, 122.98, 120.42, 120.24, 119.90, 90.17, 88.76, 65.57, 34.64, 30.83. EI-HRMS: m/z calculated for $M^{\bullet+}$ $C_{49}H_{40}$ 628.3130 found 628.3132.

Synthesis of 3c. 3c was prepared following procedure A with 1-(*tert*-butyl)-4-ethynylbenzene **1a** (1.0 mL, 5.5 mmol, 4.7 eq.), triptycene nonaflate **2c** (1.0 g, 1.17 mmol, 1 eq.), $Pd_2(dba)_3$ (6.7 mg, 7.0 μmol, 6 mol%), PPh_3 (27 mg, 11 μmol) and CuI (4.5 mg, 23 μmol) in 7 mL of degassed diisopropylamine (iPr_2NH). White solid (567 mg, 66%). ^{1}H NMR (600 MHz, CD_2Cl_2, ppm): δ 7.68 (d, 4H, J = 8.4 Hz, ArH), 7.54–7.51 (m, 8H, ArH), 7.21 (s, 2H, ArH), 7.09 (q, 4H, J = 5.4 & 2.4 Hz, ArH), 6.06 (s, 2H, triptycene-CH), 1.42 (s, 18H, –CH_3). ^{13}C NMR (150 MHz, CD_2Cl_2, ppm): δ 152.78, 147.63, 145.28, 132.00, 128.46, 126.17, 126.03, 124.45, 120.65, 119.14, 94.86, 86.67, 52.66, 35.37, 31.50. EI-HRMS: m/z calculated for $M^{\bullet+}$ $C_{44}H_{38}$ 566.2974 found 566.2976

Synthesis of TBPE (procedure B). A Schlenk tube was charged under argon with 1-bromo-4-(*tert*-butyl)benzene **4a** (0.4 mL, 2.3 mmol, 1 eq.), ethynyltrimethylsilane (**TMSA**, 0.17 mL, 1.2 mmol, 0.5 eq.), $Pd(PPh_3)_2Cl_2$ (98 mg, 0.14 mmol, 6 mol%), 1,8-diazabicyclo[5.4.0]undec-7-ene (DBU, 2.1 mL, 14 mmol), and CuI (45 mg, 0.23 mmol) in 30 mL of a degassed benzene/water mixture (2 : 3 v/v). The reaction mixture was refluxed overnight and the solvent was then evaporated under reduced pressure. The resulting residue was extracted with ethyl acetate from an aqueous solution of 10% HCl (80 mL) and the organic layer was washed with a brine solution followed by deionized water (100 mL × 2). The desired product was isolated by silica gel column chromatography, using ethyl acetate/hexane (10 : 90 v/v) as the eluent. Pale yellow solid (182 mg, 54%). ^{1}H NMR (600 MHz, CD_2Cl_2, ppm): δ 7.50 (d, 4H, J = 8.4 Hz, ArH), 7.43 (d, 4H, J = 8.4 Hz, ArH), 1.37 (s, 18H, –CH_3). ^{13}C NMR (150 MHz, CD_2Cl_2, ppm): δ 151.56, 131.15,

125.41, 120.31, 88.72, 34.66, 30.89. EI-HRMS: *m*/*z* calculated for $M^{\bullet+}$ $C_{22}H_{26}$ 290.2035 found 290.2037.

Synthesis of CPM (procedure C). A Schlenk tube was charged under argon with 9,10-dibromoanthracene **DBA** (50 mg, 0.15 mmol, 1 eq.), 1,2-bis(4-(*tert*-butyl)phenyl)ethyne **TBPE** (95 mg, 0.33 mmol, 2.2 eq.), $Pd_2(dba)_3$ (13 mg, 15 μmol, 10 mol%), Tris(*o*-tolyl)phosphine (P(*o*-tol)$_3$, 4.5 mg, 15 μmol), KOAc (73 mg, 0.75 mmol) and LiCl (13 mg, 0.3 mmol) in 5 mL of a degassed DMF/toluene solution mixture (1 : 1, v/v). The solution was refluxed overnight and the solvent was evaporated under reduced pressure. The resulting mixture was dissolved in DCM and extracted with a saturated solution of $NaHCO_3$ (50 mL × 2). The combined organic layer was washed with deionized water (100 mL × 3), concentrated, and the product was precipitated by adding acetone. The precipitate was isolated by filtration under reduced pressure over a Millipore® filter and washed exhaustively with acetone. Green solid (183 mg, 74%). ^{1}H NMR (600 MHz, CD_2Cl_2, ppm): δ 7.67 (d, 2H, J = 6.6 Hz, ArH), 7.49 (d, 2H, J = 8.6 Hz, ArH), 7.44 (s, 8H, ArH) 7.34 (t, 2H, J = 7.2 Hz, ArH), 7.30 (d, 8H, J = 2.3 Hz, ArH), 1.35 (s, 18H, –CH_3), 1.25 (s, 18H, –CH_3). ^{13}C NMR (150 MHz, CD_2Cl_2, ppm): δ 151.28, 150.44, 141.49, 139.85, 138.88, 138.77, 134.78, 132.68, 130.86, 130.39, 128.95, 128.35, 126.37, 125.74, 125.67, 125.47, 35.20, 35.03, 31.79, 31.62. EI-HRMS: *m*/*z* calculated for $M^{\bullet+}$ $C_{58}H_{58}$ 754.4538 found 754.4539.

Synthesis of polymer CPP1 (procedure D). 9,10-Dibromoanthracene **DBA** (40 mg, 0.12 mmol, 1 eq.), **3a** (60 mg, 0.12 mmol, 1 eq.), $Pd_2(dba)_3$ (10 mg, 12 μmol, 10 mol%.), P(*o*-tol)$_3$ (5 mg, 18 μmol), KOAc (58 mg, 0.6 mmol), and LiCl (10 mg, 0.25 mmol) were refluxed in 2.4 mL of a 1 : 1 DMF/toluene mixture in a Schlenk tube under argon. After 4 days of reaction, the solvent was evaporated under reduced pressure and the resulting residue was dissolved in $CHCl_3$ and extracted with a saturated solution of $NaHCO_3$ (50 mL × 2). The organic layer was washed with deionized water (100 mL × 3), concentrated, and precipitated by adding acetone. The green solid was filtered and washed with water, methanol, and acetone and then dried under vacuum. Green solid (53 mg, 86%). ^{1}H NMR (600 MHz, $CDCl_3$, ppm): δ 8.10–7.88 (m, 4H, ArH), 7.77 (bd, 2H, ArH), 7.53–7.34 (bm, 11H, ArH) and 1.43–1.36 (br, 15H, –CH_3). ^{13}C NMR (150 MHz, $CDCl_3$, ppm): δ 153.77, 149.75, 140.86, 139.74, 138.19, 137.82, 136.12, 134.26, 132.14, 130.53, 130.50, 130.04, 129.33, 128.26, 126.40, 125.82, 125.11, 119.75, 46.45, 34.60, 31.37, 26.73; GPC traces: M_w = 15 800 Da, M_n = 6600 Da, $Đ$ = 2.4; FTIR (KBr, cm^{-1}): 2960, 1626, 1436; UV-vis: (THF, 10^{-6} M), λ_{max} [nm] = 340 and 450.

Synthesis of polymer CPP2. CPP2 was prepared following procedure D with 9,10-dibromoanthracene **DBA** (53 mg, 0.16 mmol, 1 eq.), **3b** (100 mg, 0.16 mmol, 1 eq.), $Pd_2(dba)_3$ (15 mg, 16 μmol, 10 mol%.), P(*o*-tol)$_3$ (7 mg, 24 μmol), KOAc (78 mg, 0.8 mmol) and LiCl (13 mg, 0.32 mmol) which were refluxed in 3.2 mL of a 1 : 1 DMF/toluene degassed solution mixture in a Schlenk tube under argon for 4 days. Green solid (100 mg, 97%). ^{1}H NMR (600 MHz, $CDCl_3$, ppm): δ 7.86–7.64 (m, 4H, ArH), 7.33–6.96 (bm, 21H, ArH), 1.43–1.38 (br, 9H, –CH_3). ^{13}C NMR (150 MHz, $CDCl_3$, ppm): δ 150.22, 149.53, 148.96, 141.77, 140.54, 138.81, 138.12, 137.56, 136.71, 133.65, 131.87, 130.51, 130.22, 129.83, 127.82, 127.67, 127.02, 125.75, 125.02, 123.89, 119.95, 66.08, 34.58, 31.40; GPC traces: M_w = 34 300 Da, M_n = 12 800 Da, $Đ$ = 2.6; FTIR (KBr, cm^{-1}): 2964, 1682, 1428, 730; UV-vis: (THF, 10^{-6} M), λ_{max} [nm] = 340 and 450.

Synthesis of polymer CPP3. CPP3 was prepared following procedure D with 9,10-dibromoanthracene **DBA** (67 mg, 0.2 mmol, 1 eq.), **3c** (113 mg, 0.2 mmol, 1 eq.), $Pd_2(dba)_3$ (18 mg, 20 μmol, 10 mol%.), P(*o*-tol)$_3$ (9 mg, 30 μmol), KOAc (105 mg, 1.0 mmol) and LiCl (16 mg, 0.4 mmol) which were refluxed in 4 mL of a degassed 1 : 1 DMF/toluene solution mixture in a Schlenk tube under argon for 4 days. Green solid (105 mg, 91%). ^{1}H NMR (600 MHz, $CDCl_3$, ppm): δ 8.04 (br, 4H, ArH), 7.58–6.86 (bm, 17H, ArH), 5.75 (br, 2H, triptycene-CH), 1.44 (br, 9H, –CH_3). ^{13}C NMR (150 MHz, $CDCl_3$, ppm): δ 154.72, 149.84, 141.53, 140.43, 138.64, 137.19, 132.57, 132.09, 129.79, 129.71, 129.04, 128.23, 125.30, 125.12, 124.81, 120.87, 51.94, 31.52, 30.93; GPC traces: M_w = 32 200 Da, M_n = 11 600 Da, $Đ$ = 2.7; FTIR (KBr, cm^{-1}): 2960, 1432; UV-vis: (THF, 10^{-6} M), λ_{max} [nm] = 395, 445 and 470.

Results and discussion

Synthesis of comonomers

Scheme 1 shows the synthesis of the dialkyne comonomers **3a–c** *i.e.* 9,9-dimethylfluorene **3a**, spiro bifluorene **3b**, and triptycene **3c**. The aforementioned building blocks were prepared by reacting 1-(*tert*-butyl)-4-ethynylbenzene **1a** with either the dibromo derivatives **2a** and **2b** or nonaflate synthon **2c** *via* a conventional palladium-catalyzed Sonogashira cross-coupling reaction.[56] Comonomers **3a–c** were isolated in very good yields (~66–100%) and have excellent solubility in common organic solvents, namely, dichloromethane, chloroform, tetrahydrofuran, and toluene. It is noteworthy that the formation of **3a–c** was confirmed by ^{1}H- and ^{13}C-NMR spectroscopy, as well as EI-HRMS (see Fig. 3 and Fig. S1–3, S9–11, and S18–20 in the ESI†).

Fig. 1 shows the representative ^{1}H- and ^{13}C-NMR spectra of synthon **3a** which confirm the presence of all the desired

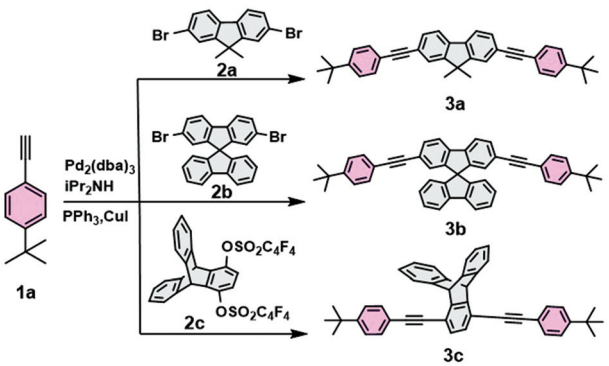

Scheme 1 Synthesis of comonomers **3a–c**.

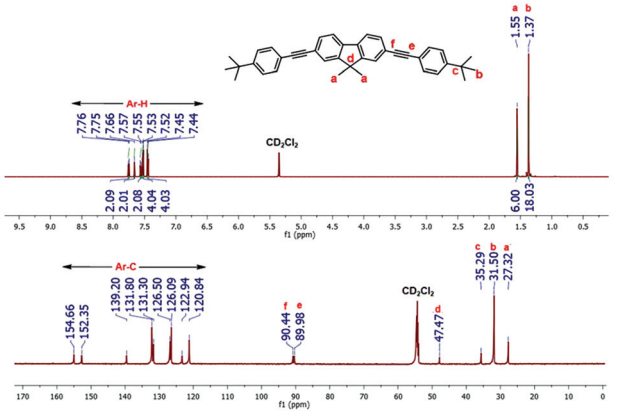

Fig. 1 ^{1}H (top) and ^{13}C (bottom) NMR of **3a** recorded in CD_2Cl_2.

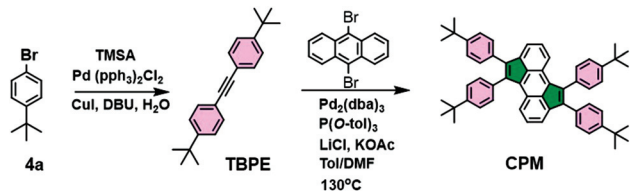

Scheme 2 Synthesis of prototypical monomer **CPM**.

peaks. All the aromatic protons and carbons of **3a** were detected in the ranges of 7.4–7.7 ppm and 120.8–154.6 ppm, respectively. The ^{1}H NMR spectrum of **3a** shows the characteristic aliphatic peaks of the methyl groups of fluorene and t-butyl moieties at 1.5 and 1.3 ppm, respectively (*cf.* peaks labeled **a** and **b** in Fig. 1). The ^{13}C NMR spectrum displays two peaks at 90.4 and 89.9 ppm, which are attributed to the characteristic sp carbons of **3a** (*cf.* peaks labeled **e** and **f** in Fig. 1). In addition, all the aliphatic peaks in the range of 47.4–27.3 ppm are in full agreement with the desired synthon **3a**. Similarly, ^{1}H- and ^{13}C-NMR spectra of comonomers **3b** and **3c** display the characteristic chemical shifts, and thus, confirm the formation of the desired products (see Fig. S1–3 and S9–11 in the ESI†). Furthermore, electron-impact high-resolution mass spectrometry (EI-HRMS) of **3a–c** reveal the formation of all the desired building blocks in high purity, as can be observed from the isotopic distribution (see Fig. S18–20 in the ESI†).

In order to prove the feasibility of the cyclopentannulation reaction, a model test was carried out by reacting 9,10-dibromoanthracene **DBA** with two equivalents of 1,2-bis(4-(*tert*-butyl)phenyl)ethyne **TBPE** in a 1 : 1 DMF/toluene mixture at 130 °C (Scheme 2) affording the prototypical target **CPM** in 74% yield.

The structure of **CPM** was confirmed by ^{1}H- and ^{13}C-NMR spectroscopy, high-resolution mass spectroscopy (HRMS), and hydrogen carbon-13 correlation 2D-NMR spectroscopy. Fig. 2 shows the ^{1}H NMR spectra of **CPM** where all the characteristic aromatic protons are revealed at 7.67 ppm (doublet, labeled **a**), 7.50 ppm (doublet, labeled **b**), and 7.34 ppm (triplet, labeled

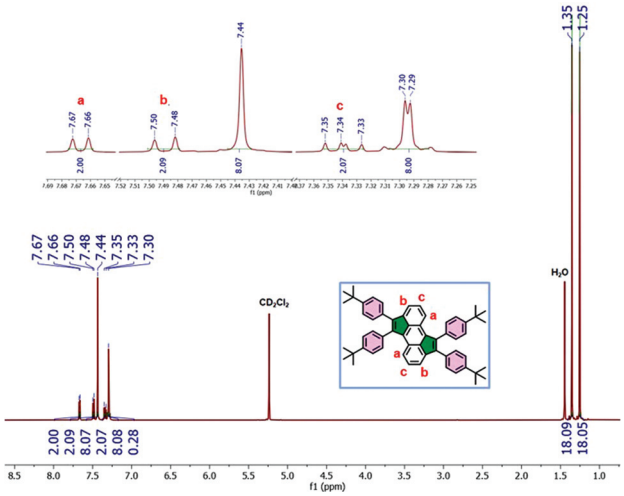

Fig. 2 ^{1}H NMR of **CPM** recorded in CD_2Cl_2.

c). The aliphatic t-butyl protons are detected at 1.35 ppm and 1.25 ppm. ^{13}C-NMR spectral analysis corroborates the above findings, and thus, further confirms the formation of the desired monomer CPM by revealing the presence of all the peaks at the expected chemical shifts. Formation of **CPM** is also supported by the 2D hydrogen carbon-13 correlation spectra which also confirm the sole formation of the desired product with the absence of any trace amount of side products (see Fig. S5, S13, and S17 in the ESI†).

The analysis of **CPM** by electron-impact high-resolution mass spectrometry (EI-HRMS) confirms its formation in high purity, as revealed by the experimentally determined isotopic patterns when compared to the calculated ones (Fig. 3).

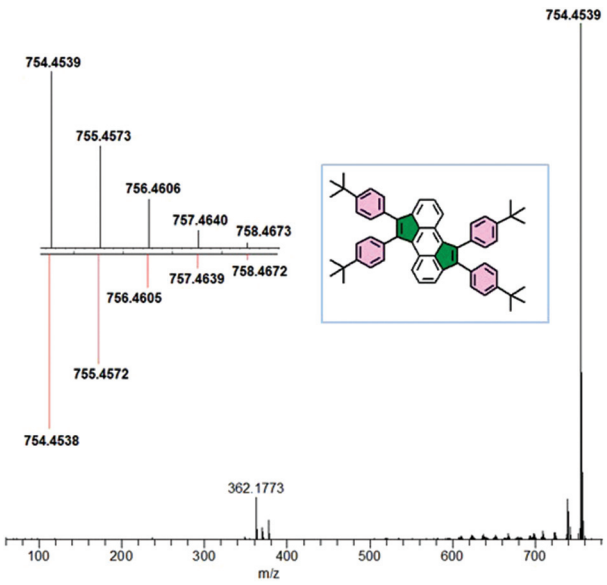

Fig. 3 EI-HRMS spectrum of **CPM**; inset: calculated (down) and measured (up) isotopic patterns of $C_{58}H_{58}^{\bullet+}$.

Synthesis of copolymers CPP1–3

As could be observed from Scheme 3, the conjugated polymers **CPP1–3** were synthesized from the cyclopentannulation reaction of **DBA** with monomers **3a–c** following the same conditions which were applied to prepare the prototypical monomer **CPM** described in Scheme 2. The polymerization was carried out by the reaction of a 0.1 M solution of **3a–c** with an equimolar amount of **DBA** in the presence of a $pd_2(dba)_3$ catalyst, a $p(o\text{-tol})_3$ ligand, a KOAc base and LiCl in a 1 : 1 DMF/toluene solvent mixture at 130 °C over four days. **CPP1–3** target polymers were isolated in excellent yields (86–97%) and were found to be highly soluble in common organic solvents such as $CHCl_3$, DCM, and THF. The high purity of **CPP1–3** was confirmed by GPC analysis, and ^{1}H- and ^{13}C-NMR, FTIR, UV-vis absorption and emission spectroscopy (see Fig. 4 and Fig. S6–8, S14–16, and S22–23 in the ESI†).

The GPC results of **CPP1–3** reveal that the average weight molar mass (M_w) ranges from 32.2 to 15.8 kDa, while the average number molecular mass (M_n) varies between 11.6 and 6.6 kDa, thus yielding polydispersity values ($Đ$) varying from 2.4 to 2.8 (Fig. 4 and Table 1, entry 1–3).

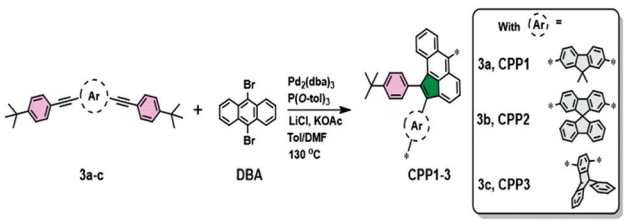

Scheme 3 Synthesis of conjugated polymers **CPP1–3**.

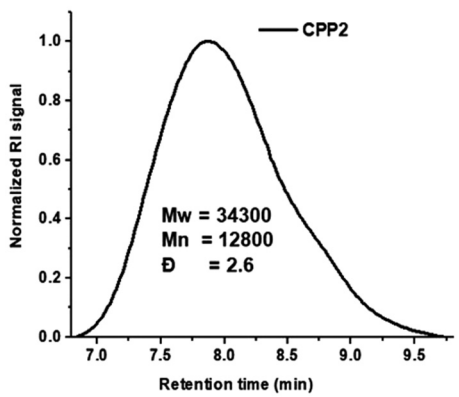

Fig. 4 Normalized GPC chromatogram of **CPP2**.

Table 1 GPC results of polymers **CPP1–3**

Entry	Product	M_w (g mol^{-1})	M_n (g mol^{-1})	$Đ$
1	**CPP1**	15 800	6600	2.4
2	**CPP2**	34 300	12 800	2.7
3	**CPP3**	32 200	11 600	2.8

Fig. 5 illustrates the comparative FT-IR absorption spectra of comonomer **3c** and its corresponding polymer **CPP3**. The characteristic stretching and bending vibrations of the aliphatic C–H groups in **3c** are observed at 2967 and 1440 cm^{-1}, respectively. In addition, **3c** divulges the characteristic C≡C stretching vibrations at 2209 cm^{-1}, which completely disappears in the FT-IR absorption spectrum of the corresponding polymer **CPP3**. The stretching and bending vibrations of the aliphatic C–H groups in CPP3 are detected at 2960 and 1432 cm^{-1}, respectively. It is noteworthy that the FT-IR spectrum of **CPP3** discloses more pronounced aromatic stretching vibrations for C–C (1400–1600 cm^{-1}) and C–H (2960–3050 cm^{-1}), when compared to those recorded for monomer **3c**. This clearly indicates the full conversion of the ethynylene moieties into the corresponding conjugated polymers.

The photophysical properties of the target polymers were measured by means of UV-Vis absorption and fluorescence spectroscopy. **CPP1** and **CPP2** display similar features with a strong UV absorption band at 340 nm, whereas **CPP3**, *i.e.* the polymer that contains triptycene units, discloses a strong absorption band at 395 nm, thus revealing a red-shift by 55 nm. Interestingly, the emission spectra of polymers **CPP1–3** show two peak maxima, the first ranging from ~403 to 433 nm, while the second being observed between 540 and 564 nm (Fig. 6).

Iodine uptake studies

Target polymers **CPP1–3** offer several advantages, namely, their contorted structures, excellent solubility, and long-range conjugation. Whilst the former property could be explained by cyclopentannulation reaction, the last two properties could be attributed to the introduction of the specially designed polycondensed aromatic hydrocarbon comonomers **3a–c**, whose spiro centers prevent the target polymers **CPP1–3** from aggregation and improve the overall polymer porosity. Therefore, the specially designed graphite-like structures of **CPP1–3** prompted us to explore their iodine adsorption and desorption properties. Vapor iodine adsorption experiments were carried out gravimetrically according to a protocol reported in the literature.[57,58] **CPP1–3** target compounds were exposed to excess iodine vapors by taking a 20 mg sample of each polymer in an open glass vial, which was in turn placed inside a sealed glass vessel that contained solid iodine at 80 °C under atmospheric pressure. The iodine uptake capacity of **CPP1–3** was monitored gravimetrically as shown in Table 2. It was observed that after one hour of iodine exposure, ~65% by weight was adsorbed by **CPP2** while half of this amount *i.e.* ~30 wt% was recorded for **CPP1** and **CPP3** (Table 2, entry 3). Subsequently, the iodine uptake by **CPP2** reached ~190 wt% after 24 hours, whereas an average of 135 wt% was recorded for **CPP1** and **CPP3** for the same exposure period (Table 2, entry 9). The adsorption values showed little increase when the polymers were kept for 72 hours, thus, suggesting the saturation of **CPP1–3**, reaching maximum iodine uptake capacities of 153, 200, and

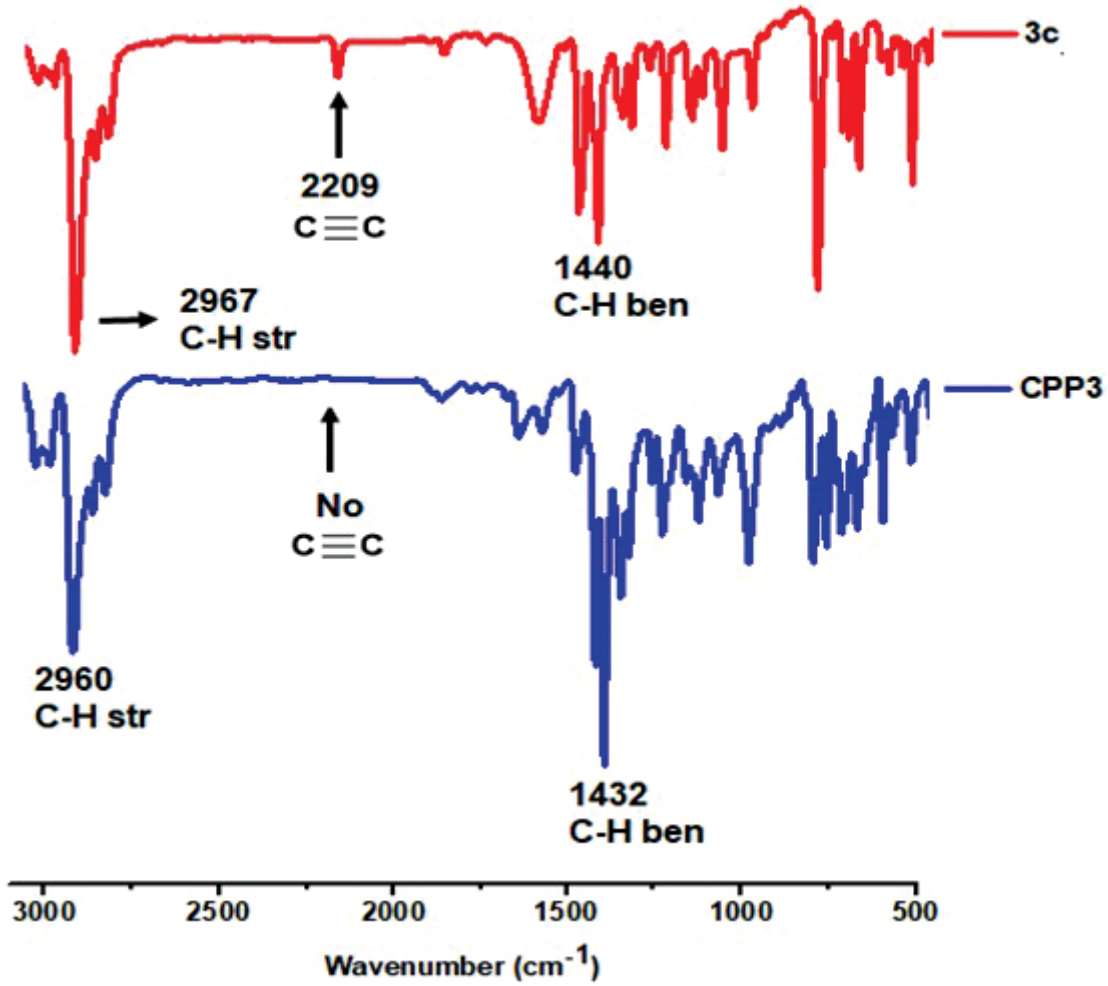

Fig. 5 Comparative FT-IR spectra of **3c** and **CPP3**.

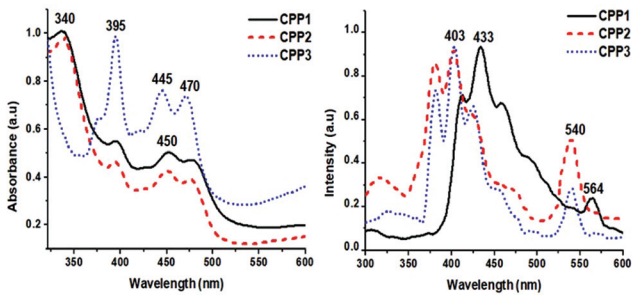

Fig. 6 Normalized UV-VIS absorption (left) and emission (right) spectra of **CPP1–3** (C_M = 10^{-6} M in THF).

Table 2 Summary of iodine adsorption of polymers **CPP1–3**

Entry	Time[a]	**CPM**[b]	**CPP1**	**CPP2**	**CPP3**	Reused **CPP2**
1	0	—	—	—	—	—
2	0.5	—	13	45	9	43
3	1	—	34	65	30	67
4	2	—	47	80	45	82
5	3	—	67	120	60	115
6	4	—	93	140	85	138
7	5	—	100	150	100	147
8	6	—	107	160	115	153
9	24	16	129	190	140	173
10	72	32	153	200	140	180

[a] Hours. [b] wt% iodine uptake.

140 wt%, respectively (Table 2, entry 10). It is noteworthy that the iodine uptake capacity of the prototypical monomer **CPM** is just 32 wt% after 72 hours of exposure to iodine vapors, which is far lower than that of its corresponding polymers **CPP1–3**.

The 200 wt% iodine uptake value of **CPP2** is superior to those of polymers reported in the literature, and notable among these are nitrogen-rich triptycene-based materials (NTP, 180 wt%),[59] calix[4]arene-based 2D macromolecules (CX4-NS, 114 wt%),[60] porphyrin and pyrene-based conjugated microporous polymers (Por-Py-CMP, 130 wt%),[61] nitrogen-containing materials (NRPPs, 192 wt%),[57] JLUE covalent organic polymer (JLUE-COP-3, up to 90.29%),[62] conjugated microporous polymers with thiophene units (SCMPs, 222 wt%),[34]

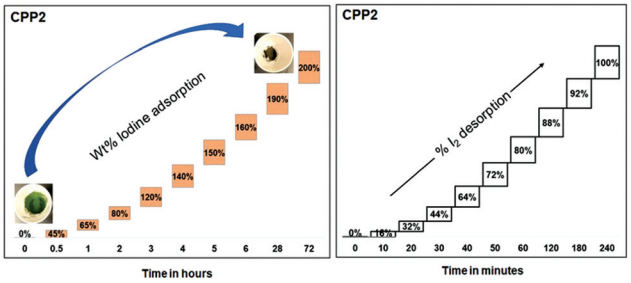

Fig. 7 CPP2 gravimetric adsorption (left) and desorption (right, heated at 125 °C in air) of iodine as a function of time. Inset: crucible photographs showing the color change after iodine adsorption.

hierarchically porous adamantane-based macromolecules (202 wt%),[63] triazine-based covalent frameworks (TTPT, 177wt%),[64] fluorine-enriched polymers (FCMP-600@1–4, up to 141 wt%)[65] and many others.[66,67]

The iodine adsorbed by **CPP1–3** could be released by simple heating of these latter polymers in air at 125 °C. The complete 100% iodine desorption efficiency for the iodine-loaded polymers (**I_2@CPP1–3**) was recorded at different time intervals (Fig. 7 and Fig. S24 and S26 in the ESI†). The reusable adsorption efficiency of the polymers was investigated using **CPP2**, which showed the maximum uptake capacity for iodine. For this, we first heated a sample of **CPP2** fully loaded with iodine vapors (**I_2@CPP2**) at 125 °C for 24 hours, in order to ensure the complete release of the adsorbate from the polymer backbone. The reactivated **CPP2** was then exposed to iodine vapors and its uptake was recorded gravimetrically using the procedure described above, revealing an uptake pattern similar to that of a freshly prepared polymer (Table 2). It is worth mentioning that **CPP1–3** undergo a color change from green/brown to black upon exposure to iodine vapors and return to their original color when heated to 125 °C in order to release the adsorbate (Fig. 7, inset).

Iodine desorption results were further supported by immersing **CPP1–3** in ethanol, an excellent solvent for dissolving iodine but not the target polymers (Fig. 8 and Fig. S25 and S27 in the ESI†). The iodine extraction in ethanol was studied by recording the UV-visible absorbance spectra at different time intervals (Fig. 8). A noticeable increase with time in the intensity of the absorbance maxima that correspond to iodine, *i.e.* ~227 nm (due to I_2), ~290 nm and ~359 nm (due to polyiodide ions), was observed which confirms the adsorbate release from **CPP2** under ambient conditions. The amount of iodine released increased rapidly within the first 20 minutes and reached equilibrium after 45 minutes. The color of the solution changed from colorless to yellow (Fig. 8) which further confirms the iodine release in ethanol. These experimental observations strongly suggest that **CPP1–3** can be employed as sorbent materials for efficient iodine vapor uptake. Moreover, once the polymers are loaded with iodine (**I_2@CPP1–3**), they can be easily regenerated either by heating or soaking in ethanol, which makes the recycling process quite practical.

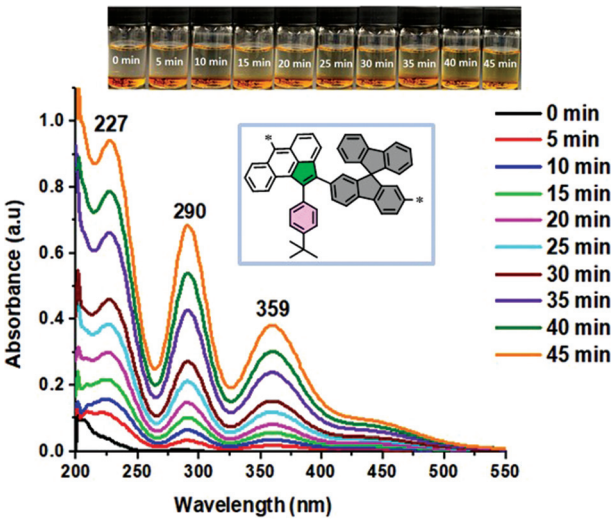

Fig. 8 UV-Vis absorption spectra upon immersion of **I_2@CPP2** in ethanol. Inset: photographs of the solutions showing a color change upon immersion in ethanol.

Conclusion

We report the synthesis of three new conjugated polymers **CPP1–3** *via* typical palladium-catalyzed cyclopentannulation reaction conditions. The target polymers, which contain contorted monomers, namely, dimethyl fluorene (**CPP1**), spirobifluorene (**CPP2**), and triptycene (**CPP3**), were isolated in excellent yields and found to have high relative weight-average molecular weights (M_w) in the range of 15.8–34.3 kDa and a polydispersity index ($Đ = M_w/M_n$) varying between 2.4 and 2.8. Iodine vapor sorption studies of **CPP1–3** reveal a high % by weight uptake that reaches 200 wt% for **CPP2** with the possibility to regenerate the polymer either by heating in ambient air or soaking in ethanol. This paves the way towards using these promising materials as versatile recyclable iodine gas adsorbents for applications in the field of environmental remediation.

Conflicts of interest

There are no conflicts to declare.

Acknowledgements

The project was partially supported by Kuwait Foundation for the Advancement of Sciences (KFAS) under project code PN18-14SC-03. We would like to thank the general facilities projects GS01/01, GS01/03, GS01/05, GS03/01, and GS03/08 at Kuwait University.

References

1 A. Leventis, J. Royakkers, A. G. Rapidis, N. Goodeal, M. K. Corpinot, J. M. Frost, D.-K. Bučar, M. O. Blunt,

F. Cacialli and H. Bronstein, *J. Am. Chem. Soc.*, 2018, **140**, 1622–1626.
2 A. Ichige, H. Saito, J. Kuwabara, T. Yasuda, J.-C. Choi and T. Kanbara, *Macromolecules*, 2018, **51**, 6782–6788.
3 M. J. Sung, S. Yoon, S.-K. Kwon, Y.-H. Kim and D. S. Chung, *ACS Appl. Mater. Interfaces*, 2016, **8**, 31172–31178.
4 J. Yang, P. Cong, L. Chen, X. Wang, J. Li, A. Tang, B. Zhang, Y. Geng and E. Zhou, *ACS Macro Lett.*, 2019, **8**, 743–748.
5 K. Aoshima, M. Nomura and A. Saeki, *ACS Omega*, 2019, **4**, 15645–15652.
6 H. Huang, H. Bin, Z. Peng, B. Qiu, C. Sun, A. Liebman-Pelaez, Z.-G. Zhang, C. Zhu, H. Ade, Z. Zhang and Y. Li, *Macromolecules*, 2018, **51**, 6028–6036.
7 J. Yuan, J. Ouyang, V. Cimrová, M. Leclerc, A. Najari and Y. Zou, *J. Mater. Chem. C*, 2017, **5**, 1858–1879.
8 S.-H. Kang, A. Jeong, H. R. Lee, J. H. Oh and C. Yang, *Chem. Mater.*, 2019, **31**, 3831–3839.
9 Y. Du, H. Yao, L. Galuska, F. Ge, X. Wang, H. Lu, G. Zhang, X. Gu and L. Qiu, *Macromolecules*, 2019, **52**, 4765–4775.
10 L. Zhang, Z. Wang, C. Duan, Z. Wang, Y. Deng, J. Xu, F. Huang and Y. Cao, *Chem. Mater.*, 2018, **30**, 8343–8351.
11 S. Shin, F. Menk, Y. Kim, J. Lim, K. Char, R. Zentel and T.-L. Choi, *J. Am. Chem. Soc.*, 2018, **140**, 6088–6094.
12 I. Choi, S. Yang and T.-L. Choi, *J. Am. Chem. Soc.*, 2018, **140**, 17218–17225.
13 F. Chen, Y. Jiang, Y. Sui, J. Zhang, H. Tian, Y. Han, Y. Deng, W. Hu and Y. Geng, *Macromolecules*, 2018, **51**, 8652–8661.
14 T. M. Swager, *Macromolecules*, 2017, **50**, 4867–4886.
15 T. Bura, S. Beaupre, M.-A. Legare, J. Quinn, E. Rochette, J. T. Blaskovits, F.-G. Fontaine, A. Pron, Y. Li and M. Leclerc, *Chem. Sci.*, 2017, **8**, 3913–3925.
16 A. Marrocchi, A. Facchetti, D. Lanari, S. Santoro and L. Vaccaro, *Chem. Sci.*, 2016, **7**, 6298–6308.
17 A. Hirose, K. Tanaka, R. Yoshii and Y. Chujo, *Polym. Chem.*, 2015, **6**, 5590–5595.
18 B. Alameddine, N. Baig, S. Shetty and S. Al-Mousawi, *Polymer*, 2019, **178**, 121589.
19 N. Baig, S. Shetty, S. Al-Mousawi, F. Al-Sagheer and B. Alameddine, *Mater. Today Chem.*, 2018, **10**, 213–220.
20 K. Aravindu, E. Cloutet, C. Brochon, G. Hadziioannou, J. Vignolle, F. Robert, D. Taton and Y. Landais, *Macromolecules*, 2018, **51**, 5852–5862.
21 Z. Wang, C. Wang, Y. Fang, H. Yuan, Y. Quan and Y. Cheng, *Polym. Chem.*, 2018, **9**, 3205–3214.
22 B. Alameddine, R. Sobhana Anju, S. Shetty, N. Baig, S. Al-Mousawi and F. Al-Sagheer, *J. Polym. Sci., Part A: Polym. Chem.*, 2017, **55**, 3565–3572.
23 C.-F. Yao, K.-L. Wang, H.-K. Huang, Y.-J. Lin, Y.-Y. Lee, C.-W. Yu, C.-J. Tsai and M. Horie, *Macromolecules*, 2017, **50**, 6924–6934.
24 X. Yan, M. Xiong, J.-T. Li, S. Zhang, Z. Ahmad, Y. Lu, Z.-Y. Wang, Z.-F. Yao, J.-Y. Wang, X. Gu and T. Lei, *J. Am. Chem. Soc.*, 2019, **141**, 20215–20221.
25 J.-S. M. Lee and A. I. Cooper, *Chem. Rev.*, 2020, **120**, 2171–2214.
26 A. Rafiee and K. R. Khalilpour, in *Polygeneration with Polystorage for Chemical and Energy Hubs*, ed. K. R. Khalilpour, Academic Press, 2019, pp. 331–372, DOI: 10.1016/B978-0-12-813306-4.00011-2.
27 S. Chu and A. Majumdar, *Nature*, 2012, **488**, 294–303.
28 B. K. Sovacool, *Util. Policy*, 2009, **17**, 288–296.
29 D. Banerjee, A. J. Cairns, J. Liu, R. K. Motkuri, S. K. Nune, C. A. Fernandez, R. Krishna, D. M. Strachan and P. K. Thallapally, *Acc. Chem. Res.*, 2015, **48**, 211–219.
30 H. Ma, J.-J. Chen, L. Tan, J.-H. Bu, Y. Zhu, B. Tan and C. Zhang, *ACS Macro Lett.*, 2016, **5**, 1039–1043.
31 D. F. Sava, K. W. Chapman, M. A. Rodriguez, J. A. Greathouse, P. S. Crozier, H. Zhao, P. J. Chupas and T. M. Nenoff, *Chem. Mater.*, 2013, **25**, 2591–2596.
32 K. W. Chapman, P. J. Chupas and T. M. Nenoff, *J. Am. Chem. Soc.*, 2010, **132**, 8897–8899.
33 Y. Lin, X. Jiang, S. T. Kim, S. B. Alahakoon, X. Hou, Z. Zhang, C. M. Thompson, R. A. Smaldone and C. Ke, *J. Am. Chem. Soc.*, 2017, **139**, 7172–7175.
34 X. Qian, Z.-Q. Zhu, H.-X. Sun, F. Ren, P. Mu, W. Liang, L. Chen and A. Li, *ACS Appl. Mater. Interfaces*, 2016, **8**, 21063–21069.
35 K. Kosaka, M. Asami, N. Kobashigawa, K. Ohkubo, H. Terada, N. Kishida and M. Akiba, *Water Res.*, 2012, **46**, 4397–4404.
36 F. Baig, K. Rangan, S. M. Eappen, S. K. Mandal and M. Sarkar, *CrystEngComm*, 2020, **22**, 751–766.
37 M. Janeta, W. Bury and S. Szafert, *ACS Appl. Mater. Interfaces*, 2018, **10**, 19964–19973.
38 X. Zhang, P. Gu, X. Li and G. Zhang, *Chem. Eng. J.*, 2017, **322**, 129–139.
39 A. Azadbakht, A. R. Abbasi and N. Noori, *J. Inorg. Organomet. Polym. Mater.*, 2016, **26**, 479–487.
40 T. Hasell, M. Schmidtmann and A. I. Cooper, *J. Am. Chem. Soc.*, 2011, **133**, 14920–14923.
41 C. Lee, S. Lee, G.-U. Kim, W. Lee and B. J. Kim, *Chem. Rev.*, 2019, **119**, 8028–8086.
42 Y. Xie, Y. Gong, M. Han, F. Zhang, Q. Peng, G. Xie and Z. Li, *Macromolecules*, 2019, **52**, 896–903.
43 K. Geng, T. He, R. Liu, K. T. Tan, Z. Li, S. Tao, Y. Gong, Q. Jiang and D. Jiang, *Chem. Rev.*, 2020, DOI: 10.1021/acs.chemrev.9b00550.
44 Y. Yano, N. Mitoma, H. Ito and K. Itami, *J. Org. Chem.*, 2020, **85**, 4–33.
45 W. Wang, H. Chen, H. Y. Zhu, Y. L. Huang and J. W. Yang, *Chem. – Asian J.*, 2017, **12**, 3016–3026.
46 I. C.-Y. Hou, Y. Hu, A. Narita and K. Müllen, *Polym. J.*, 2017, **50**, 3.
47 B. Alameddine, N. Baig, S. Shetty, S. Al-Mousawi and F. Al-Sagheer, *Polymer*, 2018, **154**, 233–240.
48 Z. Zeng, X. Shi, C. Chi, J. T. Lo, J. Casado and J. Wu, *Chem. Soc. Rev.*, 2015, **44**, 6578–6596.
49 Z.-X. Low, P. M. Budd, N. B. McKeown and D. A. Patterson, *Chem. Rev.*, 2018, **118**, 5871–5911.
50 B. Comesaña-Gándara, J. Chen, C. G. Bezzu, M. Carta, I. Rose, M.-C. Ferrari, E. Esposito, A. Fuoco, J. C. Jansen

and N. B. McKeown, *Energy Environ. Sci.*, 2019, **12**, 2733–2740.
51 D. Reinhard, W.-S. Zhang, F. Rominger, R. Curticean, I. Wacker, R. Schröder Rasmus and M. Mastalerz, *Chem. – Eur. J.*, 2018, **24**, 11433–11437.
52 I. Rose, C. G. Bezzu, M. Carta, B. Comesana-Gandara, E. Lasseuguette, M. C. Ferrari, P. Bernardo, G. Clarizia, A. Fuoco, J. C. Jansen, K. E. Hart, T. P. Liyana-Arachchi, C. M. Colina and N. B. McKeown, *Nat. Mater.*, 2017, **16**, 932–937.
53 X. Zhu, S. R. Bheemireddy, S. V. Sambasivarao, P. W. Rose, R. T. Guzman, A. G. Waltner, K. H. DuBay and K. N. Plunkett, *Macromolecules*, 2016, **49**, 127–133.
54 S. R. Bheemireddy, M. P. Hautzinger, T. Li, B. Lee and K. N. Plunkett, *J. Am. Chem. Soc.*, 2017, **139**, 5801–5807.
55 Z. Zhu and T. M. Swager, *Org. Lett.*, 2001, **3**, 3471–3474.
56 B. Alameddine, N. Baig, S. Shetty, S. Al-Mousawi and F. Al-Sagheer, *J. Polym. Sci., Part A: Polym. Chem.*, 2018, **56**, 931–937.
57 Y. H. Abdelmoaty, T.-D. Tessema, F. A. Choudhury, O. M. El-Kadri and H. M. El-Kaderi, *ACS Appl. Mater. Interfaces*, 2018, **10**, 16049–16058.
58 Y. Gao, Y. Deng, H. Tian, J. Zhang, D. Yan, Y. Geng and F. Wang, *Adv. Mater.*, 2017, **29**, 1606217.
59 R. M. Weiss, A. L. Short and T. Y. Meyer, *ACS Macro Lett.*, 2015, **4**, 1039–1043.
60 D. Shetty, T. Skorjanc, J. Raya, S. K. Sharma, I. Jahovic, K. Polychronopoulou, Z. Asfari, D. S. Han, S. Dewage, J.-C. Olsen, R. Jagannathan, S. Kirmizialtin and A. Trabolsi, *ACS Appl. Mater. Interfaces*, 2018, **10**, 17359–17365.
61 K. C. Park, J. Cho and C. Y. Lee, *RSC Adv.*, 2016, **6**, 75478–75481.
62 H. Guan, D. Zou, H. Yu, M. Liu, Z. Liu, W. Sun, F. Xu and Y. Li, *Front. Mater.*, 2019, **6**(12), DOI: 10.3389/fmats.2019.00012.
63 D. Chen, Y. Fu, W. Yu, G. Yu and C. Pan, *Chem. Eng. J.*, 2018, **334**, 900–906.
64 T. Geng, W. Zhang, Z. Zhu, G. Chen, L. Ma, S. Ye and Q. Niu, *Polym. Chem.*, 2018, **9**, 777–784.
65 G. Li, C. Yao, J. Wang and Y. Xu, *Sci. Rep.*, 2017, **7**, 13972.
66 M. Ansari, A. Alam, R. Bera, A. Hassan, S. Goswami and N. Das, *J. Environ. Chem. Eng.*, 2019, DOI: 10.1016/j.jece.2019.103558, In Press.
67 M. Liu, C. Yao, C. Liu and Y. Xu, *Sci. Rep.*, 2018, **8**, 14071.